JOURNAL OF CATALYSIS 71, 395–404 (1981)

A Method for Measuring Infrared Reflection–Absorption Spectra of Molecules Adsorbed on Low-Area Surfaces at Monolayer and Submonolayer Concentrations

W. G. GOLDEN,[1] DOUGLAS S. DUNN,[2] AND JOHN OVEREND

Department of Chemistry, University of Minnesota, Minneapolis, Minnesota 55455

Received April 3, 1981; revised June 26, 1981

Instrumentation has now been developed for the measurement of infrared reflection–absorption spectra (IRRAS); this is a very sensitive technique which can easily detect the vibrational spectra of many adsorbates at submonolayer concentrations on low-area surfaces. Furthermore, being a photons-in photons-out technique, it is capable of being applied in the presence of adsorbant molecules in the gas phase at pressures in the range 10^{-11}–10^{2} Torr and with substrate temperatures ranging from 77 to 1200 K. These features of the technique make it ideally suited to the study of surface species present during actual catalytic reactions. Details of the design and operation of an IRRAS spectrometer are described.

INTRODUCTION

Vibrational spectroscopy, because of its ability to yield molecular information which may be interpreted to enhance our understanding of adsorbate structures and bonding, has long been considered a desirable addition to the increasing number of modern surface analytical techniques which are becoming generally available and routinely applied. The substantial body of data which has been accumulated on the wavenumbers of the fundamental vibrations of a very large number of different molecules, both organic and inorganic, promises to be very helpful in the interpretation of spectra of surface species. Also, techniques have been developed over the years for the determination of intramolecular force constants from vibrational wavenumbers, and for the computation of vibrational wavenumbers from the intramolecular force constants and these promise to be useful in the interpretation of the surface spectra. Recently, electron-energy-loss spectroscopy (EELS) has been shown to be an effective way of obtaining the vibrational spectrum of a surface species. At specular angles it seems to be controlled by the same electric-dipole selection rules that determine the transitions in the infrared spectrum. Presently EELS has a much wider spectral range than does infrared and includes the wavenumber range primarily associated with substrate–adsorbate modes. It does have relatively low resolution (40–80 cm^{-1}) and appears to be restricted to operation under high-vacuum conditions. Infrared reflection–absorption spectroscopy (IRRAS), although at present, in our laboratory, limited to the wavenumber region above 1000 cm^{-1}, is nevertheless intrinsically capable of substantially higher resolution than EELS and, since it is a photons-in photons-out experiment, has no high-vacuum requirement for its operation. In recent years (*1–7*) there have been several reports of the observation of infrared spectra of adsorbates on low-area surfaces.

The basic theory on which the experiment is based was developed by Greenler (*8*), who was the first to note the advantage of using light near grazing incidence and the

[1] Present address: IBM Corporation, 5600 Cottle Rd., E41/013, San Jose, Calif. 95193.

[2] Present address: Bell Telephone Laboratories, 555 Union Blvd., Allentown, Pa 18103.

0021-9517/81/100395-10$02.00/0

large difference in the adsorption coefficients between light polarized perpendicular to the plane of reflection and that polarized parallel. Many of the experimental techniques for the direct measurement of IRRAS on low-area metal surfaces have utilized polarization modulation techniques (*9–11*) in which the intensity of the parallel and perpendicular polarized components of the radiation, I_p and I_s, were alternately detected. From Greenler's theory, such a polarization modulation gives an ac voltage at the output of the detector which is proportional to $I_p - I_s$ and, since I_p is absorbed by the surface molecules and I_s is not, this signal contains the infrared absorption spectrum of the surface species.

In this paper we describe the design of an IRRAS spectrometer with a double-modulation scheme such that, with a single detector the intensity sum $(I_p + I_s)$ and the intensity difference $(I_p - I_s)$ may simultaneously be measured. Since I_p and I_s are, on the average, attenuated to the same extent by randomly oriented molecules (gas phase or liquid phase) but only I_p is attenuated by adsorbed surface species, forming the ratio $(I_p - I_s/I_p + I_s)$ allows cancellation of the absorption by the randomly oriented species and the resulting signal contains only the IRRAS spectrum of the adsorbed surface species. We have also demonstrated that the modulation scheme effectively discriminates against sample emission and therefore the spectra of samples at elevated temperatures may be obtained. With the IRRAS spectrometer described in this paper, infrared spectra of submonolayer concentrations of molecules adsorbed on low-area surfaces in the presence of gas-phase adsorbant molecules at pressures from 10^{-11} to 10^{2} Torr and with substrate temperatures from 77 to 1200 K may be obtained in just a few minutes. It will be evident from the optical design that this technique is easily adapted to a variety of experimental configurations and the combined use of IRRAS and other surface techniques is relatively straightforward.

THE IRRAS SPECTROMETER

The schematic design of the spectrometer is illustrated in Figs. 1 and 2. Infrared radiation from a conventional infrared source is chopped by a rotating-blade chopper (frequency, ω_c) and focused at grazing incidence on the sample. The radiation reflected from the sample then passes through a photoelastic modulator and a fixed polarizer. This assembly modulates the polarization of the light which passes and, in fact, allows the parallel and perpendicular polarized components of the light to be alternately focused on the detector with a modulation frequency $2\omega_m$ (ω_m is the frequency at which the photoelastic modulator is driven). The output of the detector is then routed through two separate channels, cf., Fig. 2. In the lower channel in Fig. 2, the signal is demodulated with a lock-in amplifier tuned to a reference frequency, ω_c, and the output voltage is proportional to the light chopped at this frequency; i.e., the total radiation from the source as attenuated by the transfer function of the optics, and is therefore proportional to the total radiation throughput, $I_p + I_s$. The signal in the upper channel is first demodulated at $2\omega_m$, resulting in an output from the lock-in amplifier which oscillates at a frequency, ω_c, with an amplitude proportional to $I_p - I_s$. Further demodulation of this signal at ω_c yields a dc voltage in the upper channel

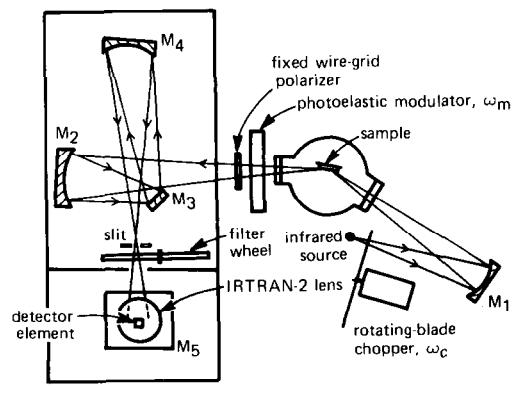

FIG. 1. Schematic diagram of the IRRAS spectrometer.

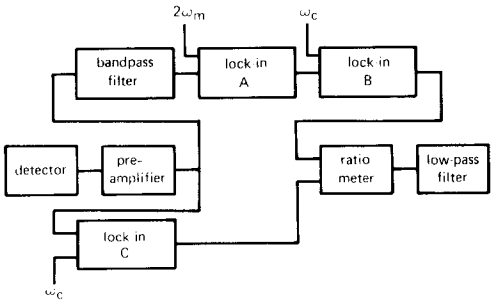

FIG. 2. Schematic diagram of the electronics for the double demodulation of the signal from the detector in the IRRAS spectrometer.

which is proportional to $I_p - I_s$.[3] The ratio of the output of the upper channel to that of the lower channel is then determined and gives a final output $(I_p - I_s)/(I_p + I_s)$.

Optical Design

The source we have used is simply a conventional infrared source taken from a Perkin–Elmer spectrometer. Sources with higher temperature and higher emissivity could be used to give enhanced signal-to-noise ratio in the experiment. The monochromator we used to obtain the spectra illustrated in this paper is a circularly variable dielectric wedge filter which has high throughput and is especially convenient for survey work. It is, unfortunately, limited in resolution to 1%, i.e., 20 cm^{-1} at 2000 cm^{-1}. Higher resolution can be achieved with relative ease, but at a sacrifice of optical throughput, by adding a grating monochromator.

Good signal-to-noise ratio is of cardinal importance in the IRRAS experiment and reasonably careful consideration of the light grasp and astigmatism of the optical design is relatively important. Figure 1 shows the general layout of the optical components. Light reflected from the sample at about $f/8$ is focused by a concave spherical mirror, M2, onto the small plane mirror, M3. The sample image is displaced only slightly off-axis in this reflection and, because M2 has diminished the beam cross section considerably, only a slightly off-axis configuration is needed for M4 to focus the sample image onto the slit and the dielectric filter. The light is finally transferred to the detector by a plane mirror, M5, angled at 45° to the optic plane and an Irtran-2 lens which brings the image of the slit to a focus on the down-looking detector. Our design is certainly not unique; many others are possible but the low cost of concave spherical mirrors makes this simple configuration quite attractive.

We used liquid-nitrogen cooled InSb (photovoltaic) and HgCdTe (photoconductive) detectors which cover the infrared spectral region from 4000 to 1000 cm^{-1}. These detectors are standard commercially available models; better detectors are available if we can solve certain problems associated with modulation frequencies and we can look forward to substantial improvements in the sensitivity and signal-to-noise ratio available in the IRRAS experiment.

The Double-Modulation Scheme

The double-modulation scheme was designed so that, with a single detector, it was possible to obtain simultaneously the intensity difference $(I_p - I_s)$ and the intensity sum $(I_p + I_s)$ of the radiation transmitted by the spectrometer. Since I_p and I_s are absorbed to exactly the same extent by randomly oriented gas-phase molecules, whereas only I_p is absorbed by the surface species, the spectrum of the gas-phase molecules cancels when the ratio $(I_p - I_s/I_p + I_s)$ is taken and only the absorption spectrum of the oriented adlayer is recorded.

The rotating-blade chopper (cf. Fig. 1) modulates the total radiation $(I_p + I_s)$ and the photoelastic modulator, fixed polarizer combination modulates the difference signal $(I_p - I_s)$. Other devices, such as a rotating polarizer or a rotating double Fresnel rhomb could be substutited for the

[3] This second demodulation at ω_c serves to improve the signal-to-noise ratio by eliminating any odd-harmonic signal components that might be passed through the first lock-in amplifier. It also allows us to discriminate against sample emission.

photoelastic modulator, fixed polarizer combination. We have experimented with these devices but have found experimental difficulties which degraded the signal-to-noise ratio and which have, to date, militated against their use.

The operational principle of the photoelastic modulator is well established (*12*) and modulators suitable for the infrared region of the spectrum have recently become commercially available. We have used a commercial zinc selenide photoelastic modulator[4] for some parts of our work and a home-built germanium one for other parts of our work; we have found both to be quite satisfactory. Briefly, the photoelastic modulator is a transparent cubic crystal which, when unstressed, has an isotropic index of refraction. A periodic strain is induced in one axis of the crystal by driving it at the frequency of its fundamental longitudinal mode and this strain results in a periodically changing refractive index for radiation polarized in that axis and hence a periodic phase retardation for radiation with that polarization.

Since we wish to modulate the experiment so that the components of radiation I_p and I_s are alternately incident on the detector, the stressed axis of the photoelastic modulator must be oriented at 45° with respect to the sample surface normal. The fixed wire-grid polarizer is oriented with its passing axis either parallel or perpendicular to the sample surface normal. The wire-grid polarizer is inserted in the optical path on the side of the photoelastic modulator remote from the sample. The advantage of this optical arrangement is that all radiation between the fixed polarizer and the detector is polarized in a particular spatial direction and the experiment is therefore insensitive to the birefringence of optical components in the spectrometer, the transfer optics and the detector.

The phase retardation, δ, induced by the photoelastic modulator is wavelength dependent, even when one neglects the wavelength dependence of the refractive index, i.e., $\delta = 2\pi d(n_y - n_x)/\lambda$, where d is the thickness of the modulator and λ is the wavelength of the radiation. Hence, in principle, the magnitude of the periodic strain induced in the photoelastic modulator must be varied with wavelength in order to produce half-wave modulation. This can be done by varying the power to the piezoelectric drivers which induce the strain in the modulator. It would be a fairly easy matter to slave the modulator power control to the wavelength drive of the monochromator and thus ensure half-wave modulation at all wavelengths. However, in practice, we have found that we do not need to vary the power to the modulator when we scan over a limited spectral range. A detailed discussion of the double-modulation scheme and its demodulation is given in an Appendix to this paper.

Optical Balancing of I_p and I_s

In practice I_p and I_s do not have equal values because of a variety of polarization effects in the optical train of the IRRAS spectrometer. The difference in intensity can be substantial (up to 10% of the total signal). It is due primarily to polarization effects in (i) the reflection coefficients of the sample, and (ii) the transmission coefficients of windows imperfectly aligned with the optic axis.

This large value of $I_p - I_s$ can consume a great deal of the possible dynamic range of the experiment and, in our experience, can reduce the sensitivity of the experiment to the point where surface species other than the most intense absorbers cannot be detected. In the double-modulation scheme it is not possible to use zero offset voltages in either the numerator or denominator channels since the resulting ratio would not be proportional to $(I_p - I_s)/(I_p + I_s)$.

The imbalance of I_p and I_s can be compensated optically by inserting an angled KBr crystal (or any other ir transparent

[4] Hinds International, Inc., P.O. Box 4327, Portland Ore 97208.

crystal) into the infrared beam. The transmission coefficients for parallel and perpendicular polarized light passing through a transparent dielectric are functions of angle of incidence and wavelength. As the angle of the KBr crystal is changed with respect to the optic axis the difference between I_p and I_s is changed and may be set to zero at any particular wavelength. Over most of the spectral region scanned this difference deviates from zero only slightly. Thus, it is possible to use much higher amplifier gains in the numerator channel and achieve maximum sensitivity.

An alternate approach, which can be used either alone or combined with the above optical compensation, involves slight modification of the zero offset circuitry of the second numerator lock-in. By substituting the attenuated output of the denominator lock-in amplifier for the constant zero-offset voltage supplied to the summing circuitry in the second numerator lock-in amplifier, multiplicative scaling of the numerator output can be achieved.

EXPERIMENTAL RESULTS

The performance of the IRRAS spectrometer described in this paper is illustrated by two examples. The first is the spectrum of CO adsorbed on a Pt (111) single-crystal substrate. The crystal was cut as a disk about 5 mm in diameter and 0.5 mm thick. This Pt (111) crystal substrate had previously been used by McCabe and Schmidt (*13*) in a study of the adsorption of CO and H_2 and had undergone several cycles of annealing *in vacuo* at 1700 K followed by oxidation in 10^{-6} Torr O_2 at 1400 K to purify the bulk of the crystal of impurities. The Pt crystal was spot-welded to two strips of tantalum foil which were in turn spot-welded to tantalum flaps on the copper posts of a uhv feed-through flange. The crystal was cleaned by heating at 1173 K in 5×10^{-7} O_2 for 15 min to remove carbon and then flashed in uhv to 1425 K to remove adsorbed oxygen. The spectrum shown in Fig. 3 is a difference spectrum

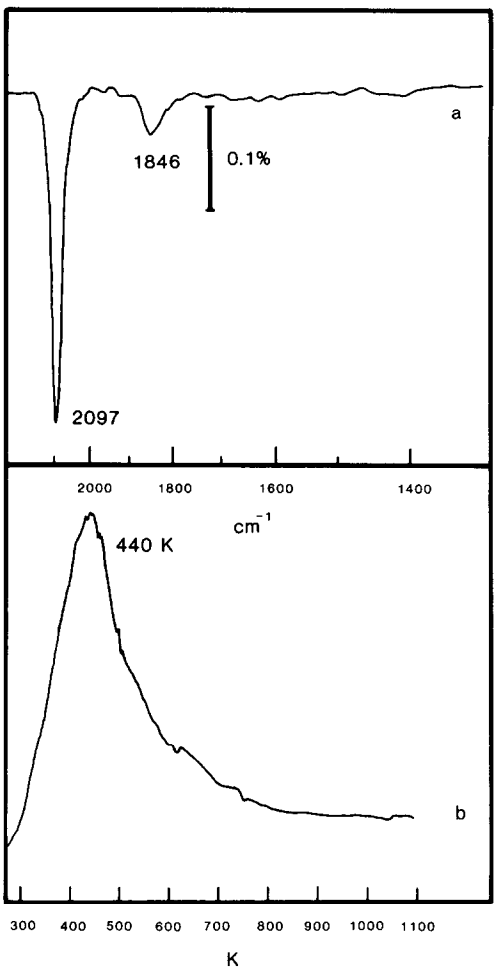

FIG. 3. (a) IRRAS spectrum of a 10-L exposure of CO to the Pt (111) crystal at 300 K. (b) TPD spectrum of the adlayer which yielded the IRRAS spectrum in (a), the heating rate was about 15 K/sec.

obtained by subtracting the IRRAS spectrum of the clean surface from the spectrum of the substrate after a 10-L exposure of CO at 300 K.

The IRRAS spectrum shown in Fig. 3 is very similar to the EELS spectrum of CO on Pt (111) reported by Froitzheim *et al.* (*14*). The absorption at 1846 cm^{-1} is clearly evident in addition to the much more intense one at 2097 cm^{-1}. This spectrum illustrates rather nicely the power of the double-modulation technique to discriminate against gas-phase absorption since there is virtually no trace of the atmo-

spheric H_2O absorption in the region of 1600 cm^{-1}, even though about 2 m of the optical path in the experiment was through an atmosphere of ordinary room air. As is well known, the absorption bands due to water vapor in such a path have absorbances as high as 50%.

As a second example of the spectra obtained with the IRRAS technique we show the spectrum of an adsorbate formed from NO on polycrystalline Pt (Fig. 4). From thermal desorption studies and by comparing the observed spectrum with the EELS spectrum reported by Gland and Gorte (*15*) we have concluded that the surface of the polycrystalline foil is primarily a reconstructed (110) surface. It is significant to note that these spectra were measured in an apparatus which was operated as a stirred tank with NO pressures from 10^{-7} to 1 Torr at a temperature of 473 K. These are conditions such as obtain in many catalytic studies and demonstrate the use of IRRAS as a tool for the study of adsorbates in reactive systems. We have operated the spectrometer with substrate temperatures ranging from 80 to 1000 K although, with the systems we have studied, we have not found spectra of adsorbates at temperatures over about 700 K; we believe that at these temperatures and under the pressures we were using virtually all the molecules were desorbed from the surface.

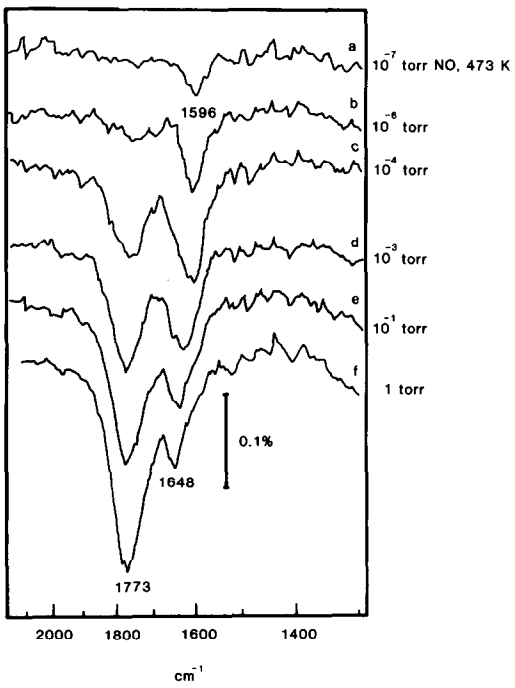

FIG. 4. IRRAS spectrum of NO adsorbate on a Pt foil with a predominantly reconstructed Pt (110) surface. This shows the changes in the adsorbate spectrum as the pressure of NO is increased in the stirred-tank sample system.

CONCLUSION

We believe that the description of the instrument and the illustrious spectra given in this paper show IRRAS to be a feasible technique for the structural study of molecular species in an adsorbate. The most attractive features of IRRAS are that it can give molecular information with regard to adsorbate–substrate systems at elevated substrate temperatures and in the presence of adsorbant molecules in the gas phase at substantial pressures. An exciting application of the IRRAS technique is to the *in situ* monitoring of adsorbate species on catalyst surfaces in gas–solid heterogeneous reactions.

The development of the spectroscopic technique is by no means complete. There are improvements in the signal-to-noise ratio which can be expected from new detectors which are becoming available and there is every expectation that the spectral range of the experiment can be extended to low wavenumbers. Within the next several years, the infrared spectra of surface species should be measurable routinely over a wavenumber range of 200–10,000 cm^{-1} under a wide variety of conditions.

APPENDIX

This Appendix gives a quantitative discussion of the production of the doubly modulated signal incident on the detector and the subsequent demodulation by the electronics of Fig. 2, to yield an IRRAS spectrum.

First, the power spectrum at the infrared detector will be derived using a derivation similar to one recently presented by Hipps and Crosby (*16*). Figure 5 shows a diagram of the PEM with a specification of the coordinate system used in the mathematical analysis. Here the PEM makes an arbitrary angle, $\pi/2 - \alpha$, with respect to the plane of reflection. The infrared source emits incoherent radiation at a particular wavelength with electric field **E** given by:

$$\mathbf{E} = \mathbf{E}_p + \mathbf{E}_s, \qquad \text{(A-1)}$$

where $\mathbf{E}_p$ and $\mathbf{E}_s$ are the components of the field oriented parallel and perpendicular to the plane of refleciton. In terms of the coordinate system in Fig. 5, $\mathbf{E}_p$ and $\mathbf{E}_s$ can be written as

$$\mathbf{E}_p = E_{0,p}(\cos\alpha\,\mathbf{i} + \sin\alpha\,\mathbf{j}), \qquad \text{(A-2)}$$

$$\mathbf{E}_s = E_{0,s}(\sin\alpha\,\mathbf{i} - \cos\alpha\,\mathbf{j}). \qquad \text{(A-3)}$$

After passing through the PEM the y component of both $\mathbf{E}_p$ and $\mathbf{E}_s$ has suffered a phase shift $\delta(t)$ with respect to the x component to produce the fields:

$$\mathbf{E}_{p,m} = E_{0,p}(\cos\alpha\,\mathbf{i} + e^{i\delta}\sin\alpha\,\mathbf{j}), \qquad \text{(A-4)}$$

$$\mathbf{E}_{s,m} = E_{0,s}(\sin\alpha\,\mathbf{i} - e^{i\delta}\cos\alpha\,\mathbf{j}) \qquad \text{(A-5)}$$

Following the PEM, the light is incident on the fixed polarizer whose passing axis is represented by the line AA in Fig. 5 and given by:

$$\mathbf{a} = \frac{1}{2^{1/2}}(\mathbf{i} + \mathbf{j}). \qquad \text{(A-6)}$$

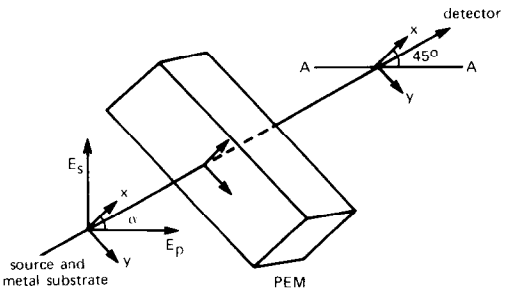

FIG. 5. Diagram of the PEM showing the coordinate system used in the derivation of the time dependence of the intensity of the light incident on the detector produced by the double modulation.

Thus the detector sees only one polarization at all times and at all wavelengths, but the detected intensity oscillates with time according to:

$$I_d = |\mathbf{a}\cdot\mathbf{E}_{p,m}|^2 + |\mathbf{a}\cdot\mathbf{E}_{s,m}|^2. \qquad \text{(A-7)}$$

Substituting the expressions for $\mathbf{E}_p$ and $\mathbf{E}_s$ from Eq. (A-4) and (A-5) gives for the detected intensity, I_d:

$$I_d = \frac{I_p + I_s}{2} + \frac{\sin 2\alpha\cos\delta}{2}(I_p - I_s), \qquad \text{(A-8)}$$

where $I_v = E_{v,0}^2$, v = s or p. Now in the PEM the relative phase shift, σ, is modulated sinusoidally between $+\delta_0$ and $-\delta_0$, where δ_0 is the maximum phase shift induced in the light beam during a period of the optical crystal's oscillation. Therefore $\delta(t)$ is given by:

$$\delta(t) = \delta_0 \sin\omega_m t, \qquad \text{(A-9)}$$

where ω_m is the modulation frequency and is equal to the frequency of the fundamental acoustic vibration of the optical crystal. The time dependence of I_d in Eq. (A-8) can then be expressed explicitly by expanding $\cos\delta(t)$ in a Fourier series (*17*):

$$\cos(\delta_o\sin\omega_m t) = J_0(\delta_0) + 2\sum_{n=1}^{\infty} J_{2n}(\delta_0)\cos(2n\omega_m t), \qquad \text{(A-10)}$$

where $J_l(\delta_0)$ is a Bessel function of integer order. In practice the series in Eq. (A-10) is truncated after the first term. Substituting Eq. (A-10) back into Eq. (A-8) gives:

$$I_d = \frac{I_p + I_s}{2} + \left(\frac{I_p + I_s}{2}\right)\sin 2\alpha\,(J_0(\delta_0) + 2J_2(\delta_0)\cos(2\omega_m t)). \qquad \text{(A-11)}$$

For convenience let $I_p + I_s \equiv I$ and $I_p - I_s \equiv \Delta I$; Eq. (A-11) then becomes

$$I_d = \frac{I}{2} + \frac{\Delta I}{2}J_0(\delta_0)\sin 2\alpha + \Delta I J_2(\delta_0)\cos(2\omega_m t)\sin 2\alpha. \qquad \text{(A-12)}$$

In addition to the polarization modulation

described above, the total light flux is also chopped at frequency ω_c by the mechanical chopper as soon as it leaves the source. When this is accounted for, the detected intensity, I_d, is given by:

$$\begin{aligned} I_d &= \frac{I}{4}(1 + \cos \omega_c t) \\ &\quad + \frac{\Delta I}{4} J_0(\delta_0)\sin 2\alpha(1 + \cos \omega_c t) \\ &\quad + \frac{\Delta I}{2} J_2(\delta_0)\cos(2\omega_m t)\sin 2\alpha(1 + \cos \omega_c t) \\ &= \frac{I}{4} + \frac{I}{4}\cos \omega_c t + \frac{\Delta I}{4} J_0(\delta_0)\sin 2\alpha \\ &\quad + \frac{\Delta I}{4} J_0(\delta_0)\sin 2\alpha \cos \omega_c t \\ &\quad + \frac{\Delta I}{2} J_2(\delta_0)\cos(2\omega_m t)\sin 2\alpha \\ &\quad \frac{\Delta I}{2} J_2(\delta_0)\cos(2\omega_m t)\sin 2\alpha \cos \omega_c t. \end{aligned} \quad \text{(A-13)}$$

(A sinusoidal shape is also assumed for this modulation since it is easier to deal with mathematically.) The above expression can be simplified by recalling that $\alpha = \pi/4$ for the IRRAS experiments (i.e., the PEM is oriented at 45° with respect to the plane of reflection) and by using the trigonometric identity:

$$\cos a \cos b = \tfrac{1}{2}\cos(a + b) + \tfrac{1}{2}\cos(a - b)$$

The expression for I_d then becomes:

$$\begin{aligned} I_d &= \frac{I}{4} + \frac{I}{4}\cos \omega_c t + \frac{\Delta I}{4} J_0(\delta_0) \\ &\quad + \frac{\Delta I}{4} J_0(\delta_0)\cos \omega_c t + \frac{\Delta I}{2} J_2(\delta_0)\cos 2\omega_m t \\ &\quad + \frac{\Delta I}{4} J_2(\delta_0)\cos(2\omega_m - \omega_c)t \\ &\quad + \frac{\Delta I}{4} J_2(\delta_0)\cos(2\omega_m + \omega_c)t. \end{aligned} \quad \text{(A-14)}$$

Equation (A-14) therefore gives the power spectrum at the detector.

In the demodulation of the upper channel, cf. Fig. 2, the bandpass filter along with the ac preamplifier of lock-in A are set to bandpass the signal out of the detector preamplifier around $2\omega_m$. These filters also pass the components of the signal at $2\omega_m \pm \omega_c$, since ω_c is small relative to $2\omega_m$. The remaining components of the signal (first four terms of Eq. A-14) are attenuated by at least a factor of 10^5, however, because of the sharp roll-off characteristics of the two filters.

Therefore the signal out of the preamplifier of lock-in A is proportional to:

$$\begin{aligned} &\frac{\Delta I}{2} J_2(\delta_0)\cos 2\omega_m t \\ &\quad + \frac{\Delta I}{4} J_2(\delta_0)\cos(2\omega_m - \omega_c)t \\ &\quad + \frac{\Delta I}{4} J_2(\delta_0)\cos(2\omega_m + \omega_c)t. \end{aligned} \quad \text{(A-15)}$$

In the demodulator circuit of lock-in A the in-phase product of the reference signal, $\cos 2\omega_m t$, is taken with the output of the preamplifier. The output of the demodulator is then switched into the low-pass filter section of the lock-in and all signal components at frequencies greater than ω_c are removed. The output of lock-in A is therefore proportional to:

$$\frac{\Delta I}{4} J_2(\delta_0) + \frac{\Delta I}{4} J_2(\delta_0) \cos \omega_c t. \quad \text{(A-16)}$$

This signal is unaltered by the input amplifier of lock-in B, except for gain, and after in-phase multiplication with the reference signal, $\cos \omega_c t$, and removal of all signal components above dc, the output of lock-in B is proportional to:

$$\frac{\Delta I}{8} J_2(\delta_0). \quad \text{(A-17)}$$

The above signal is therefore used for the numerator of the ratio.

The demodulation of the lower channel in Fig. 2 is done in a similar, but more straightforward manner. The signal out of the detector [cf. Eq. (A-14)] is first bandpassed by the input amplifier of the lock-in C to remove all signal components with frequencies different from ω_c. After in-phase multiplication with the reference signal, $\cos \omega_c t$, in the demodulator circuit and

low-pass filtering of everything above dc, the output of lock-in C is proportional to:

$$\frac{I}{8} + \frac{\Delta I}{8} J_0(\delta_0). \qquad \text{(A-18)}$$

This signal is used for the denominator input to the ratiometer. The ratiometer output is therefore proportional to the ratio:

$$\frac{\Delta I J_2(\delta_0)}{I + \Delta I J_0(\delta_0)}. \qquad \text{(A-19)}$$

So far, nothing has been said about the loss of energy of the light beam as it passes through the optical system. Let there be a general absorbance a_g (due to gas-phase molecules, infrared windows, the PEM, etc.) that is the same for both the parallel and perpendicular components, so that, by Beer's law the intensity, I, is diminished by:

$$I = I^0 e^{-a_g}. \qquad \text{(A-20)}$$

On reflection from the metal substrate the parallel and perpendicular components are absorbed to different extents, due to the adlayer, so the final light intensity is given by:

$$I_v = I_v{}^0 e^{-a_g} e^{-a_v}, \qquad \text{(A-21)}$$

where v = p or s depending on the polarization of the electric vector. Substitution of Eq. (A-21) into Eq. (A-19) gives for the ratiometer output:

$$\frac{e^{-a_g}(I_p{}^0 e^{-a_p} - I_s{}^0 e^{-a_s}) J_2(\delta_0)}{e^{-a_g}[I_p{}^0 e^{-a_p} + I_s{}^0 e^{-a_s} + J_0(\delta_0)(I_p{}^0 e^{-a_p} - I_s{}^0 e^{-a_s})]}, \qquad \text{(A-22)}$$

which shows explicitly the cancellation of the spectra of all randomly oriented absorbers leaving only the spectrum of the oriented adlayer. Since $I_p + I_s \simeq 100(I_p - I_s)$ the denominator is essentially independent of the difference between the parallel and perpendicular components yielding a simpler ratio:

$$\frac{(I_p - I_s) J_2(\delta_0)}{I_p + I_s}. \qquad \text{(A-23)}$$

As previously noted, δ_0, the maximum relative phase shift, is inversely proportional to the wavelength of the light, λ. In the experiments carried out to date δ_0 was simply set at π (half-wave retardation) for a particular wavelength in the wavelength region scanned. At shorter wavelengths the retardation was therefore greater than half-wave, while at longer wavelengths the retardation was less than half-wave. The effect of this varying retardation can be seen from Fig. 6 which shows J_2 as a function of δ_0. As can be seen from this figure and Eq. (A-23), varying δ_0 from π (half-wave retardation) simply decreases the value of the ratio (and hence the spectral sensitivity) slightly. For most of our early experiments using the Ge PEM, half-wave retardation was set at 2000 cm^{-1} which resulted in a relative sensitivity (rela-

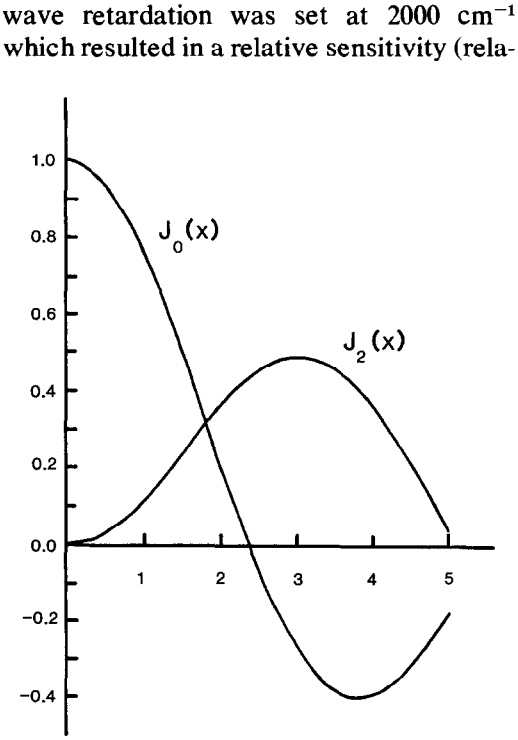

FIG. 6. Plot of the Bessel functions $J_0(x)$ and $J_2(x)$ for some values of the maximum retardation.

tive to the maximum at half-wave retardation, $\delta = \pi$) of 95% at 2200 cm^{-1} and 70% at 1250 cm^{-1}.

REFERENCES

1. SHIGEISHI, R. A., AND KING, D. A., *Surface Sci.* **58,** 379 (1976).
2. CROSSLEY, A., AND KING, D. A., *Surface Sci.* **68,** 528 (1977).
3. SHIGEISHI, R. A., AND KING, D. A., *Surface Sci.* **75,** L397 (1978).
4. GOLDEN, W. G., DUNN, D. S., PAVLIK, C. E., AND OVEREND, J., *J. Chem. Phys.* **70,** 4426 (1979).
5. ITO, M., ABE, S., AND SUËTAKA, W., *J. Catal.* **57,** 80 (1979).
6. KREBS, H. J., AND LÜTH, H., *Appl. Phys.* **14,** 337 (1977).
7. CAMPUZANO, J. C., AND GREENLER, R. G., *Surface Sci.* **83,** 301 (1979).
8. GREENLER, R. G., *J. Chem. Phys.* **44,** 310 (1966); *J. Chem. Phys.* **50,** 1963 (1968).
9. BLANKE, J. F., Ph. D. thesis, University of Minnesota, 1975.
10. CATTARICK, T., Ph. D. thesis, University of London, 1973.
11. BRADSHAW, A. M., AND HOFFMANN, F., *Surface Sci.* **52,** 449 (1975); *J. Catal.* **44,** 328, (1976).
12. CHABAY, I., Ph.D. thesis, University of Chicago, 1972; CHABAY, I., AND HOLZWARTH, G., *Appl. Opt.* **14,** 454 (1975).
13. MCCABE, R. W., AND SCHMIDT, L. D., *Surf. Sci.* **65,** 189 (1977).
14. FROITZHEIM, H., HOPSTER, H., IBACH, H., AND LEHWALD, S., *Appl. Phys.* **13,** 147 (1977).
15. GORTE, R. J., AND GLAND, J. L., *Surf. Sci.* **102,** 348 (1981).
16. HIPPS, K. W., AND CROSBY, G. A., *J. Phys. Chem.* **83,** 555 (1979).
17. ABRAMOWITZ, H., AND STEGUN, I. (Ed), "Handbook of Mathematical Functions," p. 361. National Bureau of Standards, Washington, D.C., 1972.